

# Geochemical prospecting for rare earth elements using termite mound materials

Yu Horiuchi · Tetsuji Ohno · Mihoko Hoshino ·  
Ki-Cheol Shin · Hiroyasu Murakami ·  
Maiko Tsunematsu · Yasushi Watanabe

Received: 7 October 2013 / Accepted: 13 August 2014 / Published online: 7 October 2014  
© Springer-Verlag Berlin Heidelberg 2014

**Abstract** The Blockspruit fluorite prospect, located in North West State of the Republic of South Africa, occurs within an actinolite rock zone that was emplaced into the Kenkelbos-type granite of Proterozoic age. There are a large number of termite mounds in the prospect. For geochemical prospecting for rare earth elements (REEs), in total, 200 samples of termite mound material were collected from actinolite rock and granite zones in the prospect. Geochemical analyses of these termite mound materials were conducted by two methods: portable X-ray fluorescence (XRF) spectrometry and inductively coupled plasma-mass spectrometry (ICP-MS). Comparison of the two methods broadly indicates positive correlations of REEs (La, Ce, Pr, Nd, and Y), in particular Y and La having a strong correlation. As the result of modal abundance analyses, the actinolite rock at surface mainly consists of ferro-actinolite (89.89 wt%) and includes xenotime (0.26 wt%) and monazite (0.21 wt%) grains as REE minerals. Termite mound materials from actinolite rock also contain xenotime (0.27 wt%) and monazite (0.41 wt%) grains. In addition, termite mound materials from the actinolite rock zone have high hematite and Fe silicate contents compared to those from granite zone. These relationships suggest that REE

minerals in termite mound materials originate from actinolite rock. Geochemical anomaly maps of Y, La, and Fe concentrations drawn based on the result of the portable XRF analyses show that high concentrations of these elements trend from SW to NE which broadly correspond to occurrences of actinolite body. These results indicate that termite mounds are an effective tool for REE geochemical prospecting in the study area for both light REEs and Y, but a more detailed survey is required to establish the distribution of the actinolite rock body.

**Keywords** Termite mounds · Rare earth elements · Geochemical prospecting · South Africa · Blockspruit · Portable XRF

## Introduction

Prospecting techniques for the rare earth element (REE) resources in the past were mainly geochemical prospecting of surface samples, collected along grids or lines, followed by laboratory analysis using X-ray fluorescence (XRF) and inductively coupled plasma-mass spectrometry (ICP-MS). Because these conventional methods are time consuming, we explore a new method for REE exploration: in situ chemical analysis of termite mounds using a portable XRF spectrometer, a method that is gaining credibility for the exploration of base and precious metals (e.g., Sarala 2013). Geochemical prospecting using termite mounds has traditionally been used to explore for gold, zinc, uranium, and other metals (West 1970; Watson 1972; Brooks 1982; Gleeson and Poulin 1989; Le Roux and Hambleton-Jones 1991).

The site chosen for this study was the Blockspruit fluorite prospect, which is located in a farm approximately 100 km northwest of Pretoria, Republic of South Africa (Fig. 1). The prospect area, 1,200 m×800 m in size, is a flat area about 1,150 m above sea level with a few small knolls. There are

Editorial handling: D. Huston and B. Lehmann

**Electronic supplementary material** The online version of this article (doi:10.1007/s00126-014-0550-3) contains supplementary material, which is available to authorized users.

Y. Horiuchi · T. Ohno · M. Hoshino (✉) · M. Tsunematsu ·  
Y. Watanabe  
Geological Survey of Japan, AIST, Higashi 1-1-1,  
Tsukuba 305-8567, Japan  
e-mail: hoshino-m@aist.go.jp

K.-C. Shin  
Research Institute for Humanity and Nature, Kyoto, Japan

H. Murakami  
Interdisciplinary Research Center for Catalytic Chemistry, AIST,  
Tsukuba, Japan

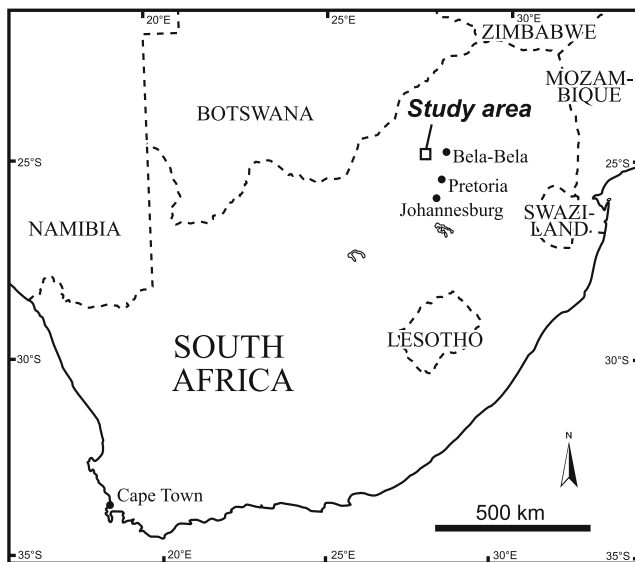


**Fig. 1** Locality map of the study area

several fluorite excavation trenches and dumps within the study area. An extensive soil and laterite cover makes the hard rock outcrops scarce.

## General geology and REE mineralization

The Blockspruit fluorite prospect is located in an actinolite body that was emplaced into the Kenkelbos-type granite of Proterozoic age (Fig. 2). This prospect contains a number of fluorite occurrences, which occur as either narrow vertical NW striking pegmatitic veins or large sheets with a nearly horizontal attitude. The largest horizontal sheets are the Ysterkop North and South bodies, which measure 1,500 and 1,000 m<sup>2</sup> in area, respectively, and have been proved by drilling to be in excess of 30 m thick (Crocker et al. 1988). The Ysterkop North and South bodies form low knolls marked by large black-colored boulders of hematite rocks, although these rocks are poorly exposed on the surface due to intense weathering and flat topography. The hematitized rocks consist of pegmatitic quartz, fluorite, and actinolite more or less completely replaced by hematite. Actinolite rocks from surface are composed of dark green to black ferro-actinolite with pinkish brown intergranular apatite crystals which are commonly replaced by hydrothermal xenotime and monazite. This results in heavy REE mineralization in the prospect (Hoshino et al. 2013).

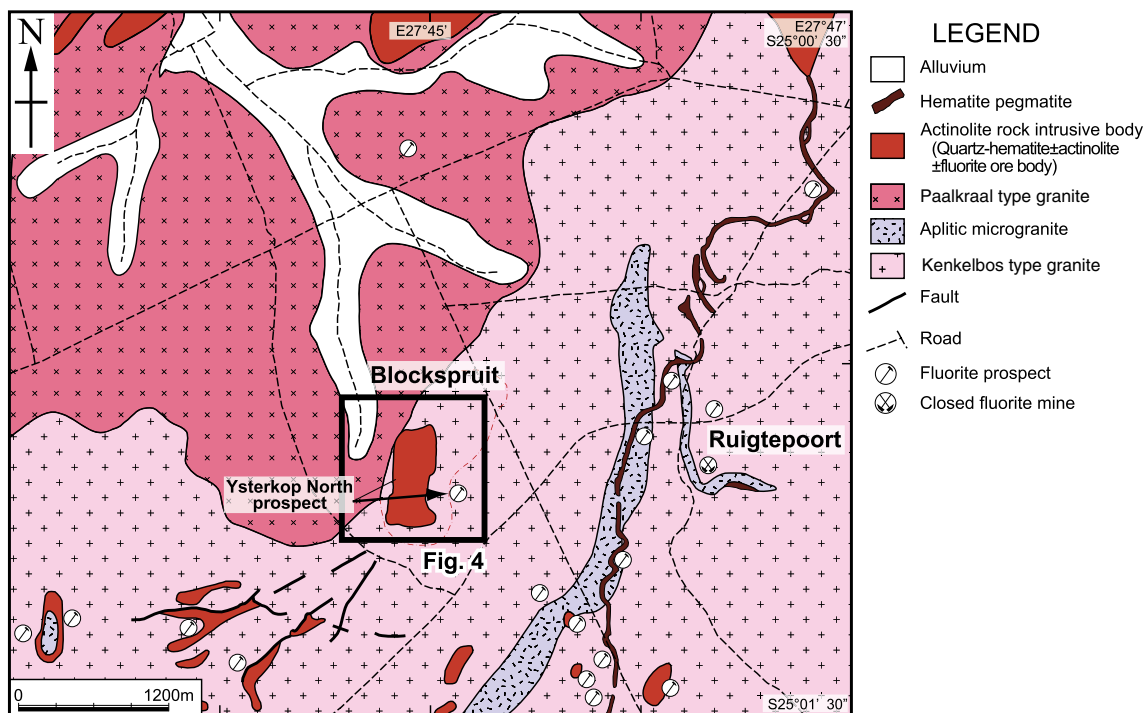


**Fig. 2** Geological map around the Blockspruit prospect (modified from Crocker et al. (2001)). The red broken line around the Ysterkop North is the outer limit of the orebody determined by

Crocker et al. (2001). Dense-colored areas in the center represent occurrence area of silicified and hematitized actinolite rock of the Ysterkop North bodies observed by this study

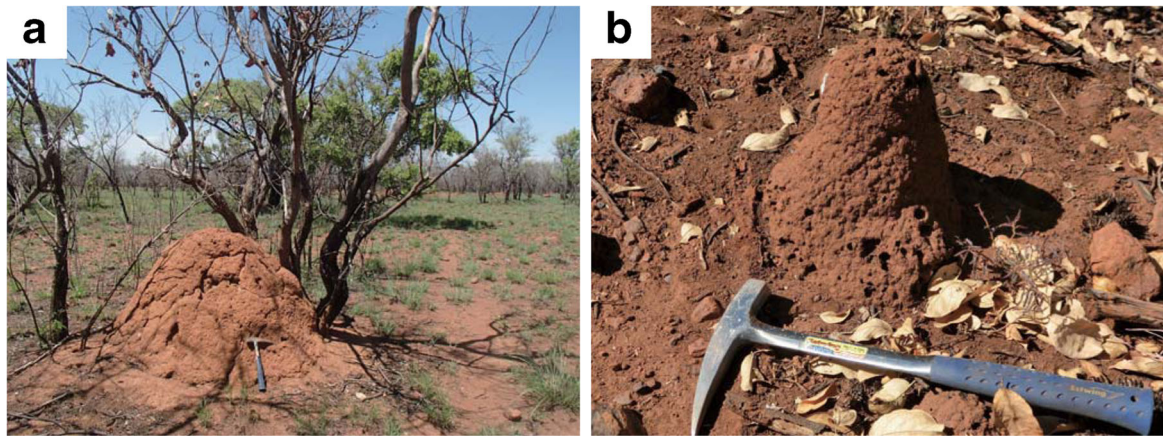


**Fig. 3** Example of typical termite mounds. **a** Large mound no. 184; **b** small mound no. 384

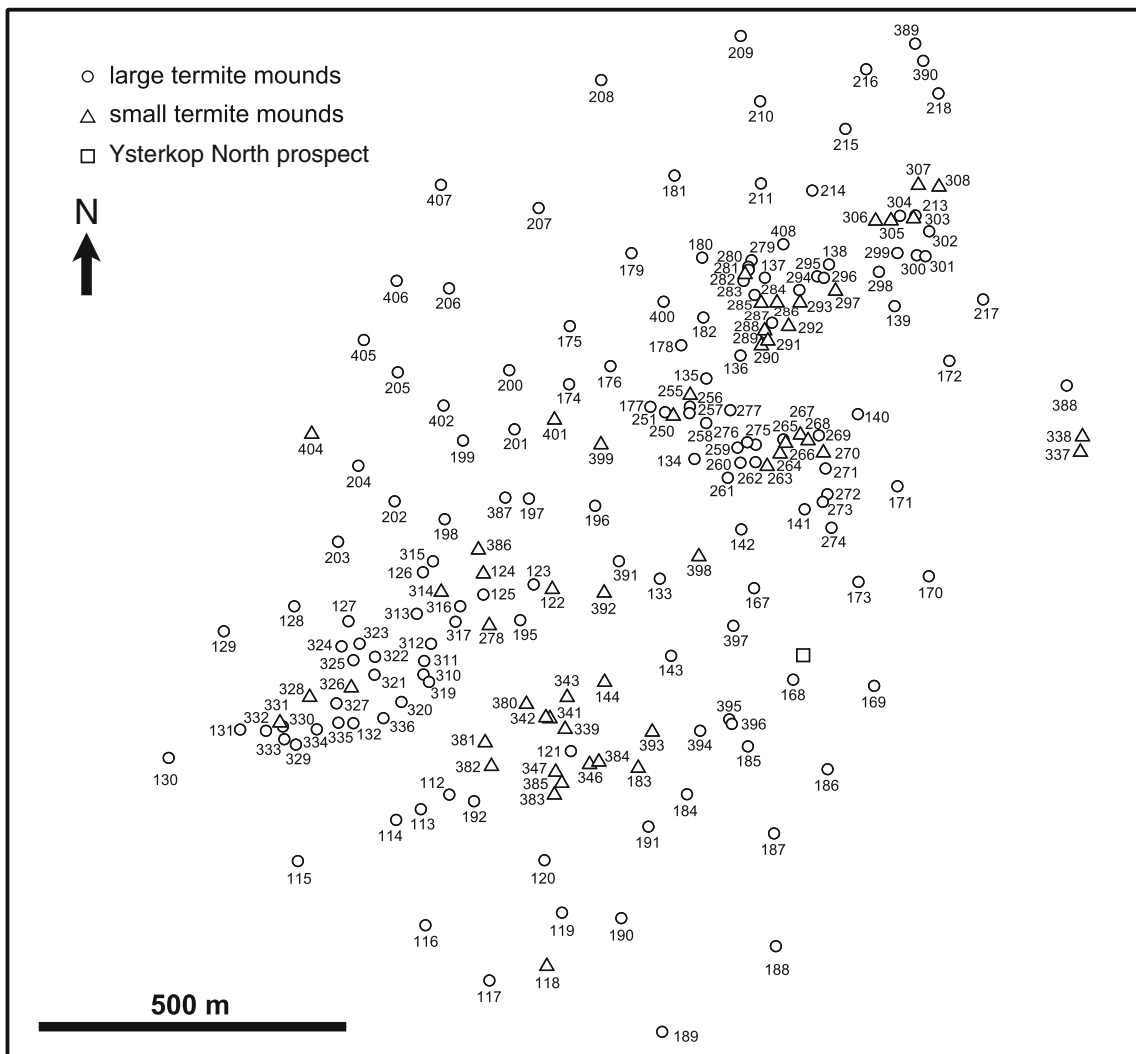


**Fig. 4** Distribution of termite mounds. Location of the map area is shown in Fig. 2

## Termite mounds

Despite poor exposure of the REE-mineralized actinolite rock, termite mounds (Fig. 3) are widely distributed over the survey area of 1,200 m×800 m (Figs. 2–4). The area is covered by savanna with sparse vegetation of acacia and bush willow trees. Although the genus and species of termites have not been identified yet, two distinct types of termite mounds occur in the survey area: large (more than a meter in diameter, Fig. 3a) and small (less than about half meter, Fig. 3b) mounds. Ferrar (1982) described termite fauna, including 20 species from 15 genera and two families at the Nylsvley Reserve, 100 km east-northeast from Blockspruit area.

The large termite mounds are commonly located under the trees (Fig. 3a). The mounds of this type are well consolidated to form a conical shape with variable heights up to 1 m from the ground. Some of the large termite mounds have a low domed shape, less than 1 m in height, and between constructed with loosely packed regolith. The large mounds are sparsely distributed throughout the survey area, although the density of distribution is not uniform (Fig. 4).

They are reddish to yellowish brown in color and composed of consolidated clay to very coarse sand-size grains that originated from the underlying actinolite rock and granite. Quartz grains are frequently observed in areas underlain by granite. Anastomosing tunnels about 3 cm in diameter were observed inside of the mounds. Some of the mounds contain living termites, and the part sampled recovered in a day. Hollows and cavities are sometimes observed on abandoned mounds, which seem to have been holed by predatory animals.

Small termite mounds (Fig. 3b) are widespread across the survey area (Fig. 4). These mounds seem to be constructed by soil-feeding termites. The mounds of this type are well consolidated, columnar domed in shape, and less than 50 cm in height. They are mostly dark brown in color and composed of consolidated clay with some sand particles. The inside of the mounds is filled with dense networking tunnels. Most of the mounds contain living termites which occasionally coexist with black ants.

## Analytical methods

For geochemical prospecting of REEs, the chemical composition of termite mound materials was measured by mining mode of a portable XRF spectrometer (Niton XL 3 t-900S-M, Thermo Scientific) in the field. A fundamental parameter (FP) method was used for corrections of chemical composition by the mining mode. In all, 147 large mounds and 53 small

mounds were investigated (Fig. 4). Multiple (four to five) samples were collected from different parts of each mound and mixed to obtain an average concentration of REEs. In addition, in order to check the variation of REE concentration in a mound, two to five samples were separately collected from four of the mounds (Fig. 5, Appendix Table 2). Most of the collected samples, especially consolidated samples, were crushed on iron plate by a hammer in the field, in order to obtain homogeneous fine sample fractions (clay to medium

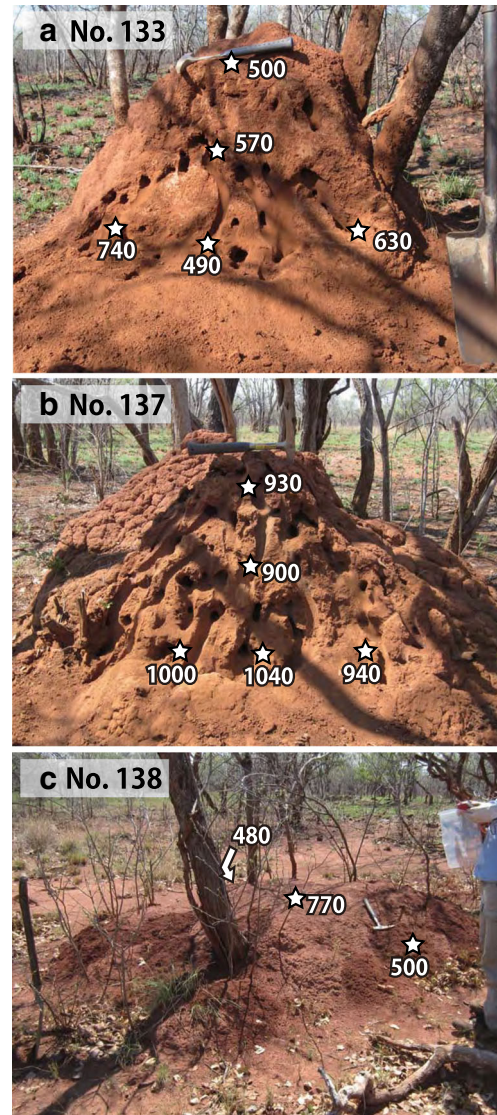


**Fig. 5** Variation of Y concentration within a termite mound measured by portable XRF spectrometer. Numbers are Y concentration (ppm). **a, b** Cutting section of mounds nos. 133 and 137; **c** surface of mound no. 138

sand size) as much as possible. The weight of the obtained samples was about 50 g. The collected samples were placed in plastic bags and measured by portable XRF spectrometer through plastic bags for about 60 to 90 s. Sizes (length, width, and height) and location of each mound were recorded to investigate the size-related REE concentration and to produce geochemical anomaly maps of REE. In addition to several major elements such as Si, Al, and Fe, five REEs (Y, La, Ce, Pr, and Nd) were analyzed.

The collected samples were subsequently brought back to the laboratory of the Geological Survey of Japan, AIST, where they were dried in an oven and pulverized. Associated minerals of their samples were identified by powder X-ray diffraction (PXRD) and the Mineral Liberation Analyzer™ (MLA).

In PXRD analysis, all samples were X-rayed with Cu-K $\alpha_1$  radiation (40 kV, 200 mA) using a Rigaku SmartLab X-ray diffractometer with D/tex Ultra detector at the Geological Survey of Japan.

Modal abundance of the representative three samples (two termite mound samples from actinolite rock and granite zones, and an actinolite rock sample) is primarily done using MLA. This instrument consists of an FEI Quanta 250 scanning electron microscope with field emission type electron gun equipped with one Bruker

nitrogen-free energy-dispersive X-ray detector (SDD detector). An actinolite rock sample collected from the surface is analyzed by the GXMAP (areal mapping) mode of the MLA, while termite mound materials from actinolite rock and granite zones by the XMOD (lattice mapping) mode.

Contents of major and trace elements of 93 samples were analyzed by ICP-MS, and their F content were also determined by ion-selective electrode (ISE) at the ActLabs commercial laboratory in Ancaster, Canada.

## Results

Figure 6 shows powder X-ray diffraction (PXRD) patterns of the termite mound materials. The termite mound materials from the actinolite rock zone mainly consist of quartz, goethite, and clay minerals, while those from the granite area consist of quartz, microcline, albite, and clay minerals.

Table 1 shows the modal abundances of minerals of the actinolite rock from the surface, termite mound materials from the actinolite and granite zones measured by MLA. Actinolite rock from the surface mainly consists of ferro-actinolite (89.89 wt%) and contains 0.26 wt%

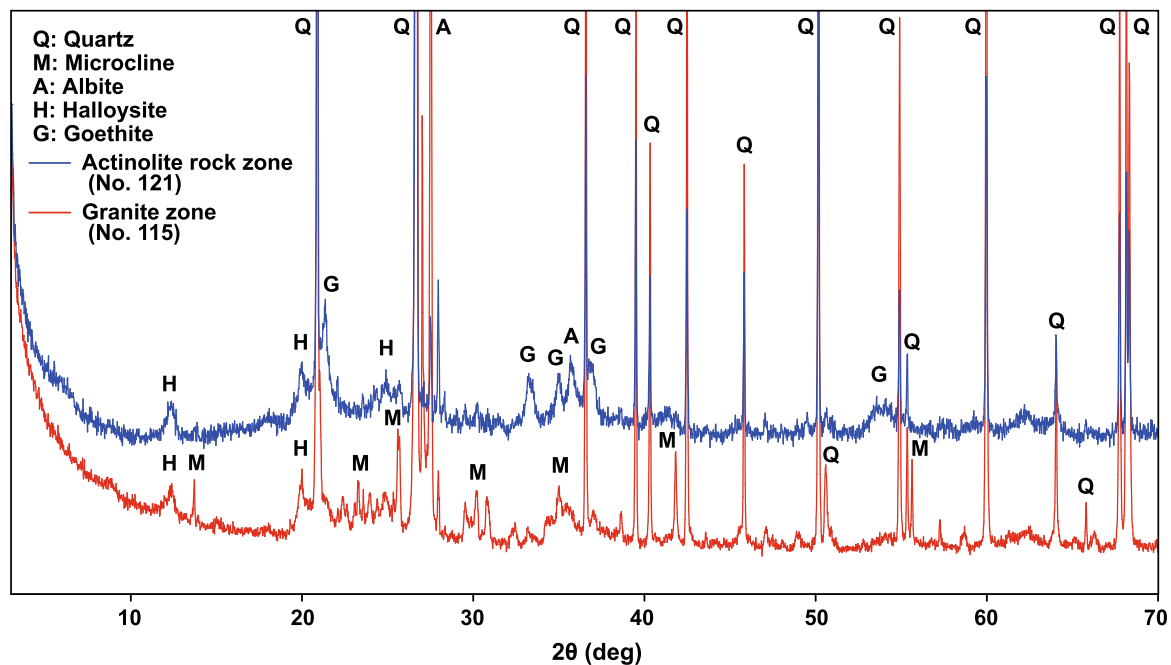


**Fig. 6** X-ray diffraction pattern of typical termite mounds. The *upper* is from actinolite rock zone. The *lower* is from granite zone

**Table 1** Modal abundances of minerals measured by MLA

Mineral	Actinolite rock (wt%)	Termite mound no. 121 from actinolite zone (wt%)	Termite mound no. 115 from granite zone (wt%)
Xenotime-(Y)	0.26	0.27	0.13
Monazite	0.21	0.41	0.01
REE Ti-oxide	0.00	0.21	0.00
cerianite	0.00	0.01	0.00
CeAlFe silicate	0.03	0.03	0.02
Th silicate	0.27	0.06	0.05
Zircon	0.00	0.06	0.13
Fluorite	0.21	0.61	0.00
Hematite	5.79	5.66	0.66
Ilmenorutile	0.00	0.12	0.14
Ilmenite	0.00	0.08	0.16
Mn oxide	0.00	0.02	0.00
FeAl silicate	0.00	39.03	46.15
Fe silicate	0.42	18.64	8.17
FeTi silicate	0.01	0.29	0.22
Annite	0.06	2.88	0.99
Ferro-actinolite	89.89	0.19	0.15
Halloysite	0.00	0.04	0.09
Quartz	0.24	24.82	36.39
Albite	0.01	1.81	1.29
Orthoclase	0.00	3.61	2.76
Montmorillonite?	0.00	0.23	0.14
Muscovite	0.00	0.88	2.34
Plagioclase	0.00	0.01	0.01
Apatite	1.93	0.01	0.00
REE-rich apatite	0.50	0.01	0.01
Unknown	0.17	0.00	0.00
Total	100.00	100.00	100.00

xenotime, 0.21 wt% monazite, and 0.5 wt% REE-rich apatite. Termite mound material from actinolite rock zone contains 0.27 wt% xenotime, 0.41 wt% monazite, 0.21 wt% REE-Ti oxide, 0.01 wt% cerianite, and 0.01 wt% REE-rich apatite, while that from granite zone includes 0.13 wt% xenotime, 0.01 wt% monazite, and 0.01 wt% REE-rich apatite. The termite mound material from actinolite rock zone shows higher modal abundance of REE minerals compared to that from granite zone. Modal abundance of the termite mound material from

actinolite rock zone, especially REE mineral, is similar to that of actinolite rock from the surface.

The data by portable XRF spectrometer and ICP-MS measurements are listed in [Electronic Supplementary Material](#). Total REE (Y, La, Ce, Pr, and Nd) concentrations range from 860 to 6,410 ppm measured by a portable XRF spectrometer and from 176 to 6,510 ppm by ICP-MS. Silicon and Al contents determined by the portable XRF spectrometer are unreliable due to absorption of characteristic X-ray of those elements by plastic bag. Therefore, Si concentration is less than 5.9 % by the portable XRF spectrometer, while from 27.1 to 41.2 % by ICP-MS. Aluminum concentration is less than 0.9 % by the portable XRF spectrometer, and from 2.2 to 6.2 % by ICP-MS. Iron concentration varies from 0.9 to 13.5 % by the portable XRF spectrometer and from 1.4 to 12.8 % by ICP-MS.

## Discussion

Availability of REE geochemical prospecting using termite mounds and behavior of REEs and relationship with other elements

Gleeson and Poulin (1989) surveyed Au distribution patterns in a mound and showed that high gold content was identified in the central portions of the termite mound, but the Au-concentrated zones also appear to be present in the upper surfaces of the mounds and in places, on the flanks. In our study, the Y content of the termite mound no. 137 in the central deep portion of the mound is high compared with the upper surface, while the Y content of no. 133 is lower (Fig. 5a, b). The Y contents of the surface samples of termite mound no. 138 are variable and do not show any regularity (Fig. 5c). There appear to be no trend of Y concentration in a termite mound, but analyzed sample numbers are few compared to those of Gleeson and Poulin (1989).

According to West (1970), the termite *Macrotermes natalensis* forages sands and follows fractures to access moisture, where the main water table depth has been estimated to be 60–90 m around the Leopard gold mine, near the village of Silobela, Zimbabwe. On the way back, they carry gold if gold-bearing quartz reef is located along their pathway (West 1970). *M. natalensis*, which builds conical mounds averaging 140 cm in basal diameter, is reported also from South African savanna

area (Ferrari 1982) and likely to be distributed in the Blockspruit area. As suggested from the example of Zimbabwe, the termites in large mounds, including the *Macrotermes* group, seem to carry deeper sediments than those of small mounds. In order to clarify the differences of Y contents between large and small termite mound materials by portable XRF, their Y anomaly maps were drawn, respectively (Fig. 7). As the result, there is no significant difference between Y anomaly maps drawn from large and small termite mound materials. The Y anomaly areas broadly correspond to occurrences of actinolite rock body (Figs. 2 and 7). These suggest that both large and small termite mound materials are efficient for geochemical prospecting for rare earth elements.

As the result of MLA measurement, the modal abundance of minerals of a termite mound located in the actinolite rock zone is clearly different from that in the granite area (Table 1). Iron-bearing minerals such as hematite and Fe silicates are dominant in termite mounds in the actinolite rock zone compared to those from the granite area. It is likely that the ferro-actinolite contained in the actinolite rock zone was decomposed to Fe silicate in termite mounds, which is reflected in a very low percentage (0.19 %) of actinolite in the termite mound (Table 1). The termite mounds in the actinolite zone have similar proportions of REE minerals such as xenotime and monazite to those of the actinolite rock zone. Moreover, the correlations between Y and F, Y

and  $P_2O_5$ , La and F, and La and  $P_2O_5$ , measured by ICP-MS, show that Y and La concentrations are obviously correlated positively with  $P_2O_5$ , but not with F (Fig. 8). Although several fluorite prospecting trenches occur in the survey area, REE mineralization seems to be related to phosphate minerals such as monazite and xenotime originating in actinolite rocks, rather than fluorite.

Figure 9a, b, c shows geochemical anomaly maps of Y, La, and Fe concentrations in the survey area, as measured by the portable XRF spectrometer. Yttrium, La, and Fe concentrations from SW to NE direction are present and broadly correspond to occurrences of actinolite rock body (Fig. 9). Several Y anomalies are detected in the north-eastern part of the survey area (Fig. 9a). However, degrees of La and Fe anomalies are low compared to those of Y anomalies (Fig. 9). This may be due to chemical varieties of actinolite rocks.

#### Reliability of REE concentration measured by portable XRF spectrometer

The results of measurements by a portable XRF spectrometer and ICP-MS were compared (Fig. 10). The results of Y and La show good correlations between these two methods, although the values of La by the portable XRF spectrometer are slightly higher. These results show that the effects of the sample preparation

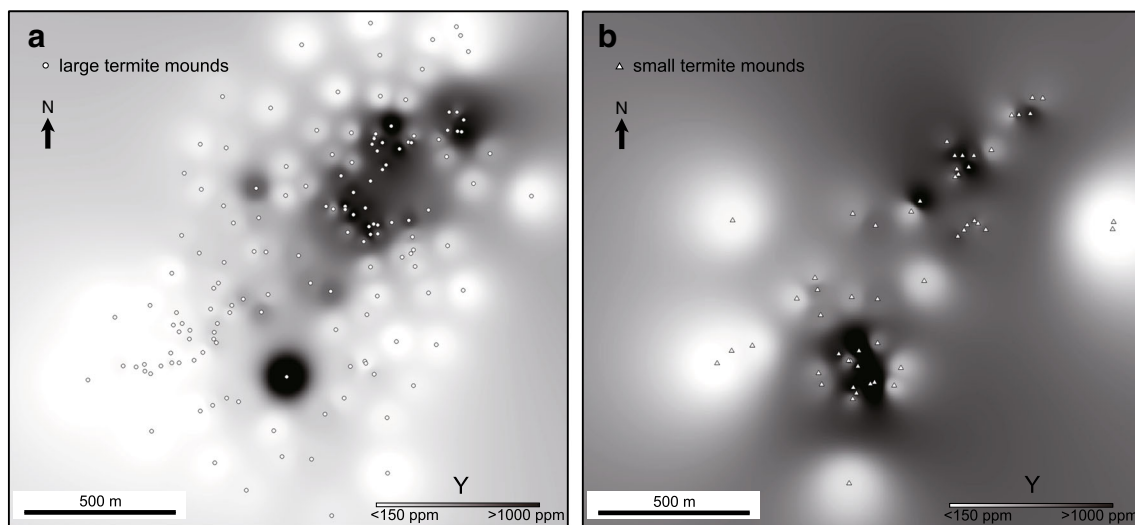


**Fig. 7** Geochemical anomaly maps of Y concentration in the survey area, measured by portable XRF spectrometer. **a** Using large termite mounds; **b** using small termite mounds. Maps were made by inverse distance weighting (IDW) interpolation method, using a distance coefficient ( $P$  value) of 3

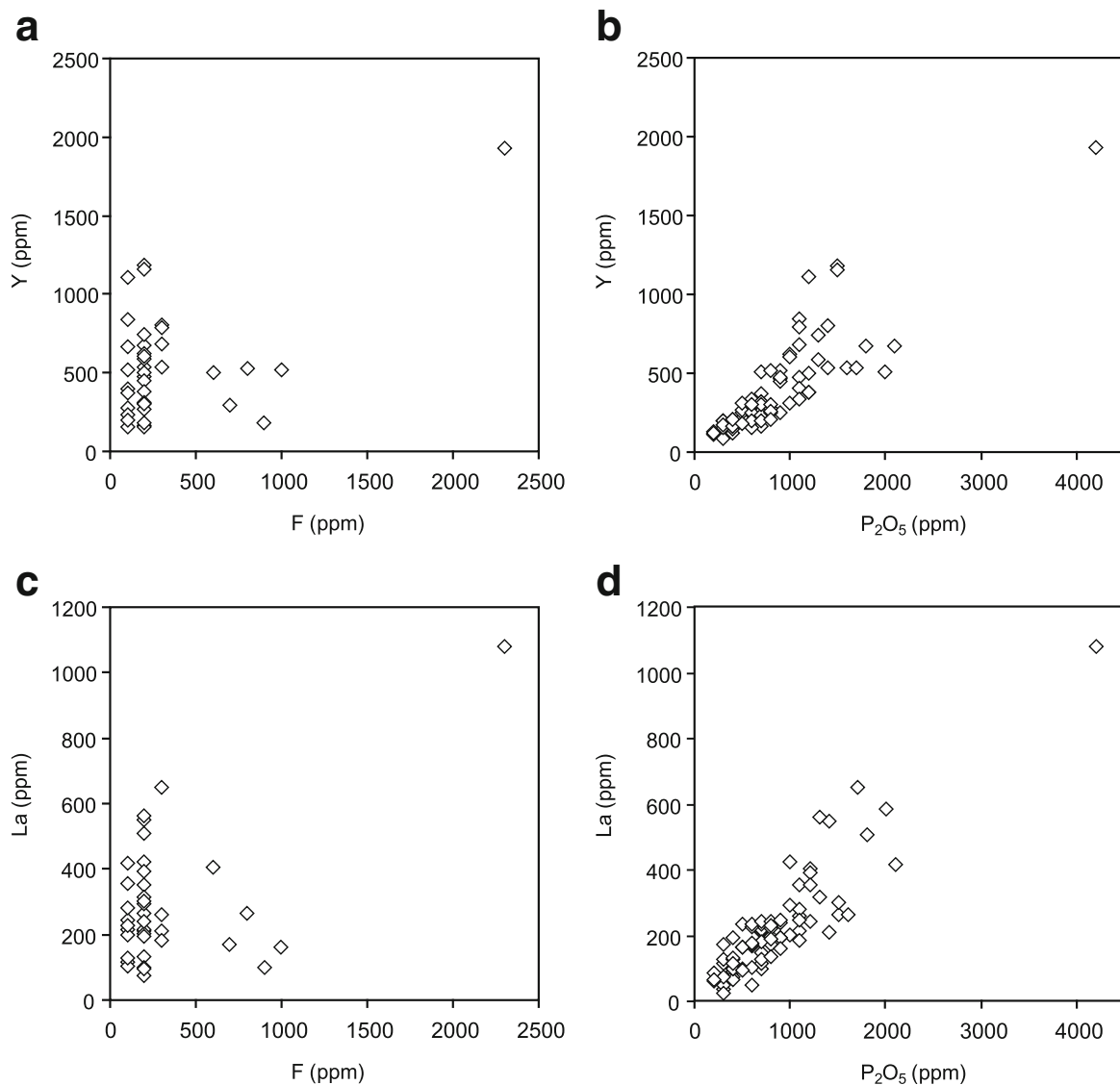


**Fig. 8** Graphs shows relation between Y or La and other elements, measured by ICP-MS. **a** Relationship between Y and F; **b** relationship between Y and P<sub>2</sub>O<sub>5</sub>; **c** relationship between La and F; **d** Relationship between La and P<sub>2</sub>O<sub>5</sub>

methods (crushing only by hammer versus drying and pulverization in the laboratory) and analytical conditions (direct sample analysis through plastic bags in the field versus complete digestion of the samples by lithium metaborate fusion method in the laboratory) are negligible.

The values of Ce are relatively scattered. The Pr and Nd values by the portable XRF spectrometer are higher than those by ICP-MS. This discrepancy may be caused by peak interferences of REEs and other elements. The L $\beta$  peak of Ba interferes with L $\alpha$  of Ce, the L $\beta$  peak

of La interferes with the L $\alpha$  peak of Pr, and the L $\beta$  peak of Ce interferes with L $\alpha$  peak of Nd. The L $\alpha$  peaks of La and the K $\alpha$  of Y were interfered by the L $\beta$  peak of Cs and K $\beta$  peak of Rb, respectively. The Ba (average (av.) 380 ppm), La (av. 235 ppm), and Ce (av. 540 ppm) contents of the studied samples are higher than Cs (av. 2.2 ppm) and Rb (av. 130 ppm) contents. Thus, Ce, Pr, and Nd values measured by the portable XRF are different from the contents measured by ICP-MS. In conclusion, Y and La values by a portable XRF



spectrometer are most reliable for REE prospecting in the survey area. Measurement of Y contents is useful for estimation of heavy REE contents, especially for Dy in the sample because of a good correlation between Y and Dy, while measurement of La is recommended for light REEs. The distributions of high Y anomaly zones drawn based on the results of portable XRF spectrometer and ICP-MS measurements are similar (Fig. 11). Although detection limits of Y and La are varied according to duration time of the measurement and the chemical composition of the samples, they are generally less than 100 ppm. These results show that the

geochemical prospecting using termite mounds by portable XRF spectrometer is practical for the quick estimation of underground distribution of REE-mineralized zones, but more detailed studies are needed to determine the exact distribution of the actinolite rock body.

## Conclusions

The comparison of two measurement methods (portable XRF spectrometer and ICP-MS) for REE concentrations of termite mound materials in the Blockspruit area

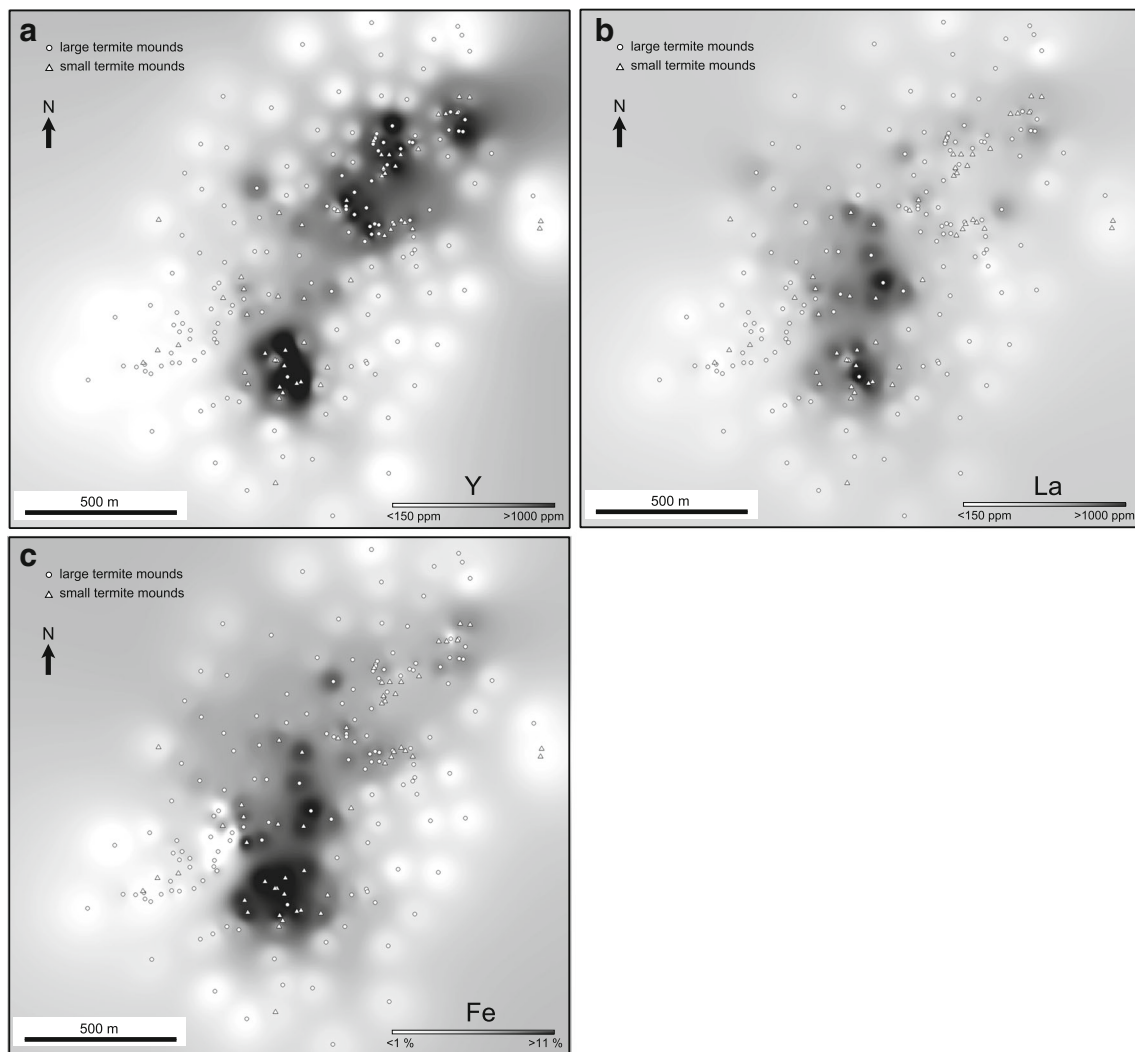


**Fig. 9** Geochemical anomaly maps of Y, La, and Fe concentrations in the survey area, measured by portable XRF spectrometer. **a** Anomaly map of Y; **b** anomaly map of La; **c** anomaly map of Fe. Maps were made by

inverse distance weighting (IDW) interpolation method, using a distance coefficient ( $P$  value) of 3

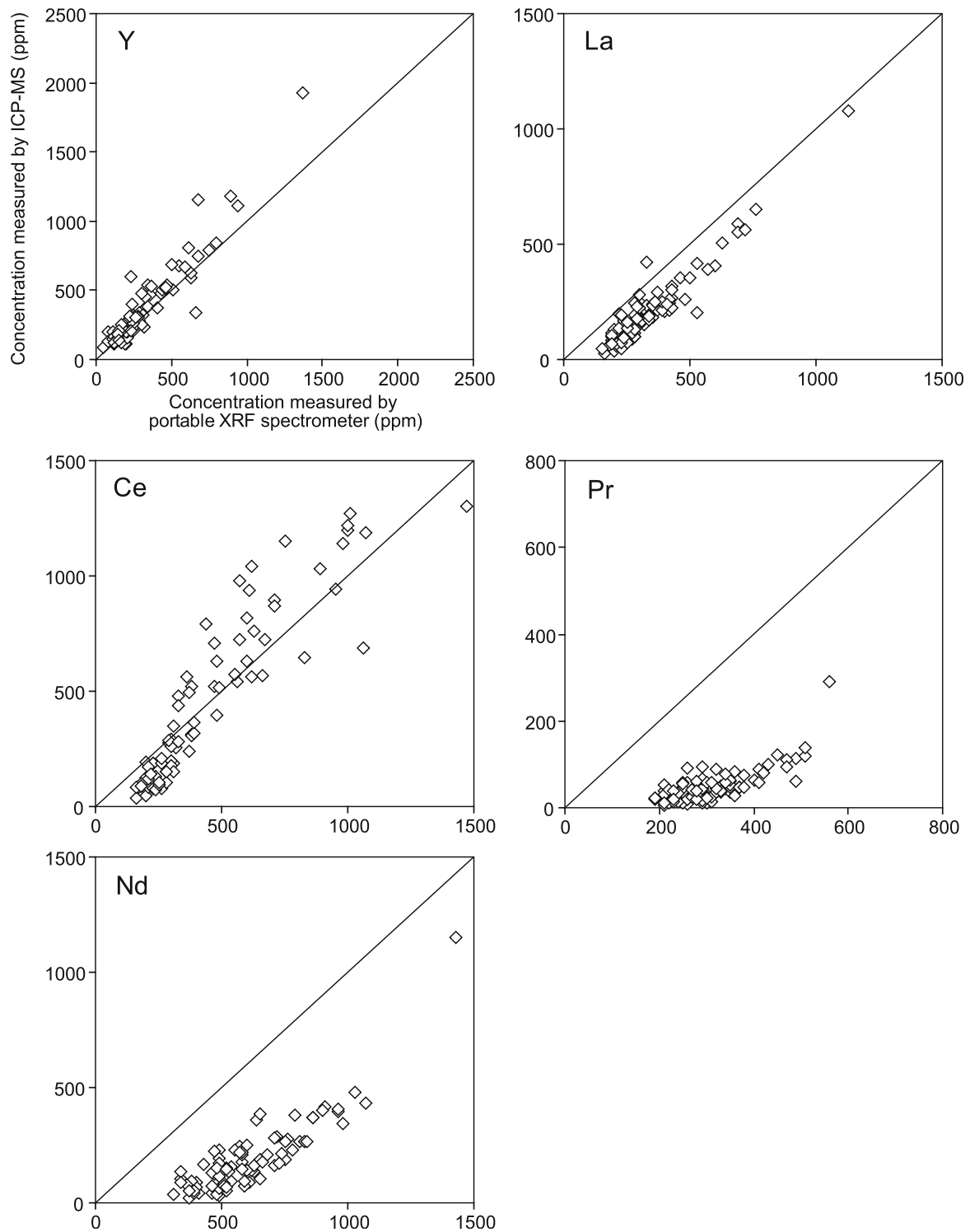


**Fig. 10** Comparison of result from portable XRF spectrometer and ICP-MS on REE concentration

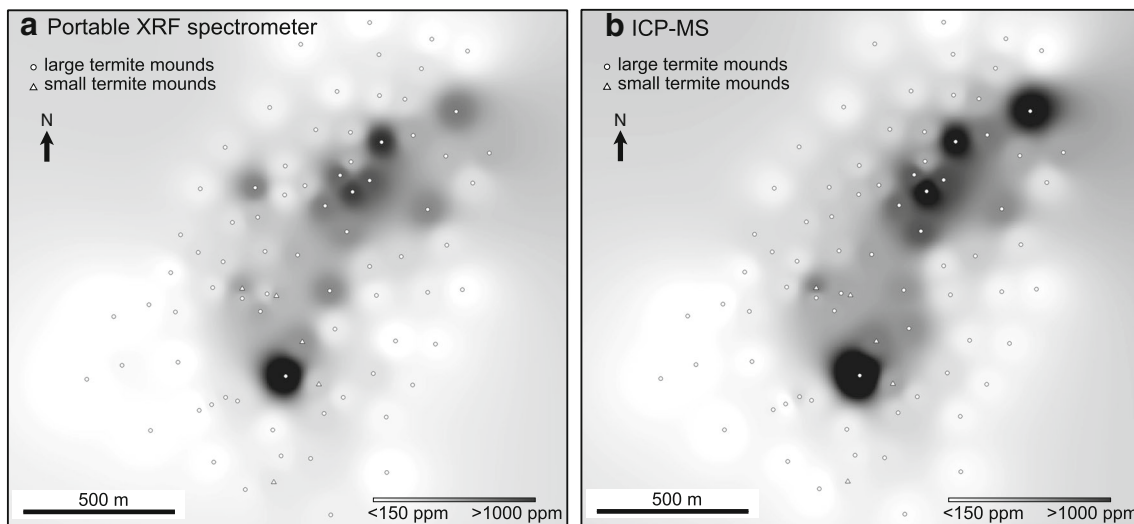


**Fig. 11** Distribution of Y concentration measured by **a** portable XRF spectrometer and **b** ICP-MS in the survey area. Maps were made by inverse distance weighting (IDW) interpolation method, using a distance coefficient ( $P$  value) of 3

confirmed that La and Y concentrations are well correlated between the two methods. The mapping results by both methods revealed the presence of several similar Y anomalies trending NE-SW in the survey area which correspond to occurrences of actinolite rocks. Therefore, the geochemical investigation using termite mounds by portable XRF spectrometer is useful for REE prospecting.

**Acknowledgements** We are grateful to Dr. Elisa Longa Tongu (Council for Geoscience, Republic of South Africa) for supporting our fieldwork in South Africa, to Dr. Akira Imai (Akita University, Japan) for revising a draft version of the manuscript, and to Dr. Masatsugu Ogasawara (Geological Survey of Japan) for suggesting technique of XRF analysis. This manuscript was significantly improved by the reviews of an anonymous reviewer and Editor-in-Chief Prof. B. Lehmann and Associate Editor Dr. D. Huston.

## References

- Brooks RR (1982) Biological methods of prospecting for gold. *J Geochem Explor* 17:109–122
- Crocker IT, Martini JEJ, Söhngge APG (1988) The fluorspar deposits of the Republics of South Africa and Bophuthatswana, Handbook 11. Geological Survey of South Africa
- Crocker IT, Eales HV, Ehlers DL (2001) The fluorite, cassiterite and sulphide deposits associated with the acid rocks of the Bushveld Complex. Memoir 90, Council for Geoscience, Pretoria, South Africa, pp115
- Ferrari P (1982) Termites of a South African savanna. I. List of species and subhabitat preferences. *Oecologia (Berl)* 52:125–132
- Gleeson CF, Poulin R (1989) Gold exploration in Niger using soils and termitaria. *J Geochem Explor* 31:253–283
- Hoshino M, Watanabe Y, Tsunematsu M (2013) Rare earth minerals in amphibolites from Blockspruit fluorite deposit, the Republic of South Africa. *Rare Earths* 62, Rare Earth Society of Japan, 94–95. (in Japanese with English abstract)
- Le Roux JP, Hambleton-Jones BB (1991) The analysis of termite hills to locate uranium mineralization in the Karoo Basin of South Africa. *J Geochem Explor* 41:341–347
- Sarala P (2013) Portable XRF methods in till geochemical exploration—examples from Finland. Extended abstracts of SGA2013 Conference, Uppsala, Sweden, 437–439
- Watson JP (1972) The distribution of gold in termite mounds and soils at a gold anomaly in Kalahari sand. *Soil Sci* 113:317–321
- West WF (1970) The Bulawayo symposium papers: no. 2, termite prospecting. *Chamb Mines J* 12:32–35